Surface diffusion of K on Pd{111}: Coverage dependence of the diffusion coefficient determined with the Boltzmann–Matano method

Cite as: J. Chem. Phys. **108**, 4212 (1998); https://doi.org/10.1063/1.475819
Submitted: 17 September 1997 . Accepted: 02 December 1997 . Published Online: 04 June 1998

M. Šnábl, M. Ondřejček, V. Cháb, Z. Chvoj, W. Stenzel, H. Conrad, and A. M. Bradshaw

Surface diffusion of K on Pd{111}: Coverage dependence of the diffusion coefficient determined with the Boltzmann–Matano method

M. Šnábl and M. Ondřejček
Fritz-Haber-Institut der Max-Planck-Gesellschaft, Faradayweg 4-6, 14195 Berlin (Dahlem), Germany and Institute of Physics, Czech Academy of Science, Cukrovarnická 10, 162 00 Praha 6, Czech Republic

V. Cháb and Z. Chvoj
Institute of Physics, Czech Academy of Science, Cukrovarnická, 10, 162 00 Praha 6, Czech Republic

W. Stenzel, H. Conrad, and A. M. Bradshaw
Fritz-Haber Institut der Max-Planck-Gesellschaft, Faradayweg 4-6, 14195 Berlin (Dahlem), Germany

(Received 17 September 1997; accepted 2 December 1997)

The surface diffusion of potassium on Pd{111} has been studied with photoelectron emission microscopy (PEEM) for coverages up to one monolayer. The coverage dependence of the chemical diffusion coefficient is determined by analysis of the concentration profiles obtained from the PEEM images with the Boltzmann–Matano method. The diffusion coefficient, D, decreases with increasing coverage but a local maximum is found at a coverage of $\Theta \approx 0.5$ ML. The values of D at low coverages ($\Theta < 0.3$ ML) agree well with those obtained in a previous investigation for $\Theta \approx 0.12$ ML. The maximum in D is interpreted in terms of an order–disorder phase transition in the adsorbed layer. © *1998 American Institute of Physics.* [S0021-9606(98)01210-0]

I. INTRODUCTION

Experimental investigations of surface diffusion show large discrepancies between the measured kinetic parameters, even for apparently identical systems (see Ref. 1 for a rather complete survey up to 1990). In spite of increasing activity in the field of surface diffusion initiated by new techniques, such as scanning tunnelling microscopy (STM), PEEM or quasielastic He scattering, it is still not clear whether the large differences in the diffusion coefficient are due to unknown artefacts associated with the particular experimental method, or whether the different techniques in fact measure different physical quantities.[1] With regard to the length scale and the number of particles involved, the experimental methods may be classified as microscopic or macroscopic. In the former, single particle jumps on an atomic scale are monitored and thus the tracer diffusion coefficient is obtained. In the latter, a substantial mass transport over macroscopic distances is measured, i.e., the chemical diffusion coefficient is determined. While the tracer diffusion coefficient describes the random walk motion of a particle at constant concentration, the chemical diffusion coefficient also includes the chemical potential of the adsorbed layer. There is, in fact, no simple relation between the two, but the Darken equation is usually assumed to be valid and they are then related via the so-called thermodynamic factor.[1] The tracer diffusion coefficient is usually derived from direct observation of single particle motion with, for example field ion microscopy (FIM) or STM, in contrast to the chemical diffusion coefficient which is commonly obtained by analyzing the evolution of non-equilibrium concentration distributions with, for example laser induced desorption (LITD), the change in work function ($\Delta\varphi$) or PEEM. These involve, by definition, significant variations of the concentration on the macroscopic scale. Since in most cases the diffusion coefficient depends on coverage, measured concentration profiles can be analyzed with the Boltzmann–Matano method[2] which (with certain restrictions, as discussed below) allows the diffusion coefficient to vary with concentration. It has been successfully applied for example by Butz and Wagner for O diffusion on W(110),[3] by Sigula and Henzler for Ag diffusion on Ge{111}[4] and by Milne *et al.* for the system Si{100}-Cs at low coverages.[5]

A critical point with all macroscopic methods is the assumption that either the substrate area used for the measurements represents a perfect surface or that defects do not influence the results. We have previously shown, however, how defect structures strongly impede diffusion.[6,7] By employing photoemission electron microscopy (PEEM) with a lateral resolution intermediate between that of the microscopic and macroscopic methods, the diffusion of potassium atoms on Pd{111} was monitored. Two-dimensional real-time images clearly showed that at low temperatures the motion of potassium out of an area precovered with K proceeds along terraces confined by steps or step bunches, thus forming quasi-one-dimensional ''streamers.'' Only at higher temperatures was diffusion over steps found to occur. At low potassium coverages ($\Theta < 0.12$ ML, Ref. 8) we determined from the temperature dependence of the diffusion coefficient an activation energy $E_d = 0.066$ eV.[9] A similarly low value, $E_d = 0.051$ eV, has been found with quasi-elastic He scattering for the diffusion of Na on Cu{100},[10] showing that the activation energies of alkali metal diffusion are probably much lower than the values obtained in previous experiments[1] and indicating the importance of accounting for the influence of surface defects in such investigations.

The coverage dependence of the diffusion coefficient is governed by the changes in lateral interactions which frequently lead in turn to the formation of ordered layers. In

consequence, complicated concentration profiles in the diffusion zone may occur, an effect which has been observed in the presence of adsorbate phase transitions (e.g., in the systems Ba on Mo{110} and W{110}, Ref. 11). For alkali metal layers the charge redistribution between adsorbate and substrate gives rise to repulsive interactions within the adsorbed layer and often leads to the formation of ordered structures, as noted in Ref. 12. The occurrence of a terrace-like region in the concentration profile of the Pd{111}-K system at 0.5 ML was reported in our previous paper.[7] Here, we show that such a feature is due to a local maximum in the diffusion coefficient at that particular coverage and that it coincides with the appearance of a $p(2\times2)$ LEED pattern. Moreover, we present a quantitative analysis of the concentration dependence of the surface diffusion coefficient calculated by means of the Boltzmann–Matano method for the whole coverage range up to 1 ML.

II. EXPERIMENTAL AND COVERAGE CALIBRATION

The experiments were performed in a UHV system equipped with a flange-on, relatively low resolution photoelectron microscope,[12] an argon-sputter-gun for surface cleaning, a rear-view LEED optics for structure characterization and a SAES getter source for K deposition.[6] The base pressure was below 10^{-10} mbar. The Pd crystal was cut to within 0.5° of the ⟨111⟩ orientation, mechanically and chemically polished and subsequently cleaned *in situ* with standard recipes. Potassium was deposited on selected areas through a slit (100 μm × 5 mm) in a metal mask which produces a strip-like initial concentration distribution. Its spatial evolution as a function of temperature up to 195 K was observed in real time and subsequently analyzed. The PEEM images on the phosphorous screen were recorded with a CCD camera and stored on magnetic tape. The CCD camera was operated in constant contrast mode which allows (after calibration) any gray level to be associated with a definite work function value throughout the entire experiment. The image processing was performed with commercial computer image and data analyzing programs.

Coverage was calibrated as follows (in Ref. 7 it was described only briefly): The clean Pd crystal was exposed at 100 K without the mask to a constant flux of K for different time intervals. After each dose, the crystal was annealed to $T\sim450$ and subsequently to 600 K, and the PEEM image intensity recorded. At about half a monolayer, corresponding roughly to the work function minimum, the 450 K annealing gives rise to a well-developed $p(2\times2)$ LEED structure in agreement to our previous results.[7] In addition, between 0.7 and 1.0 ML a $(\sqrt{3}\times\sqrt{3})$R30° ordered phase was formed. The higher coverage structure was not observed after the 600 K treatment due to a partial desorption of potassium, in agreement with data for Pd{100}-K.[13] This sequence of phases is very similar to that obtained for the Pt{111}-K system.[14] The corresponding work function changes were estimated by using a series of cut-off filters inserted sequentially in the illumination path from a Hg discharge lamp acting as light source. By noting the cut-off wavelength which suppressed any photoelectron emission, the absolute work function could be correlated with coverage. The dependence of work function on K coverage obtained in this way agrees very well with the corresponding curve for the system Pt{111}-K (Ref. 15) measured with the vibrating capacitor. The work function curve for the system Pd{111}-K has not yet been measured independently.

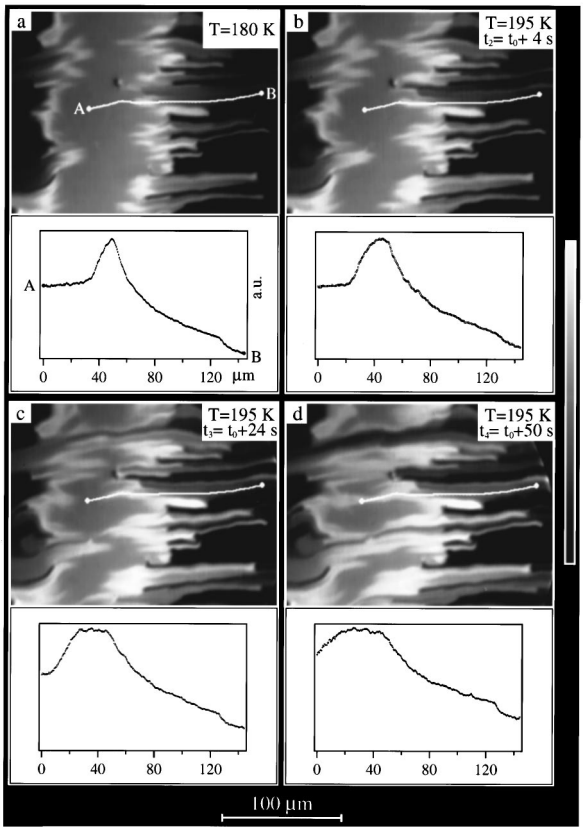

FIG. 1. PEEM images of a 1.0 ML potassium strip deposited on the clean surface of Pd{111}. The diffusion already starts at $T=100$ K. The intensity profiles below each picture are plotted along one selected streamer (indicated by the line connecting A and B).

III. RESULTS AND DATA ANALYSIS

A. Concentration profiles

As reported in our previous paper,[7] diffusion of K out of the deposition area is observed to occur even at 100 K, the lowest sample temperature accessible in our set-up. Every experimental run was therefore performed as follows: After deposition of 1 ML potassium through the slit mask at 100 K the position of the sample was adjusted in front of the microscope in order to optimize the imaging conditions. Subsequently, the substrate was heated to a temperature slightly below the measuring temperature and the K distribution observed was taken as starting configuration. The temperature then only had to be raised by a relatively small amount to the constant temperature required for the measurements. A representative distribution at 180 K is shown in Fig. 1a. The clean Pd{111} surface appears as dark areas; the gray level at position A corresponds to 1 ML potassium coverage. It should be recalled that the work function versus coverage relation for alkali metals shows a minimum, and thus the

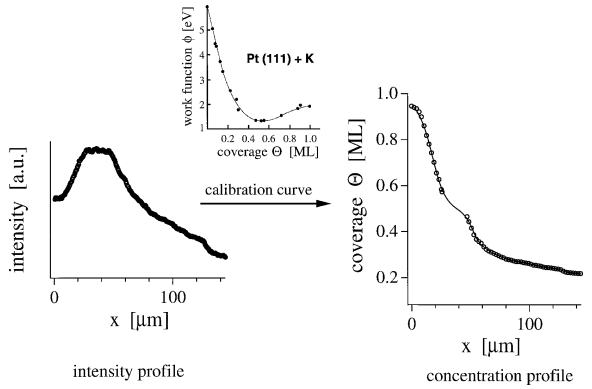

FIG. 2. Transformation of an intensity profile $I(x)$ (in this case measured at $t=t_3$) into the corresponding concentration profile $\Theta(x)$. The intensity at a position x^* is converted into the corresponding coverage Θ^* (left) by using the relationship between work function and coverage shown in the center (after Ref. 15) which serves as a normalized, inverted calibration curve. Repeating the procedure for all coverages Θ^* and positions x^* yields the curve $\Theta(x)$ (right). See text for details.

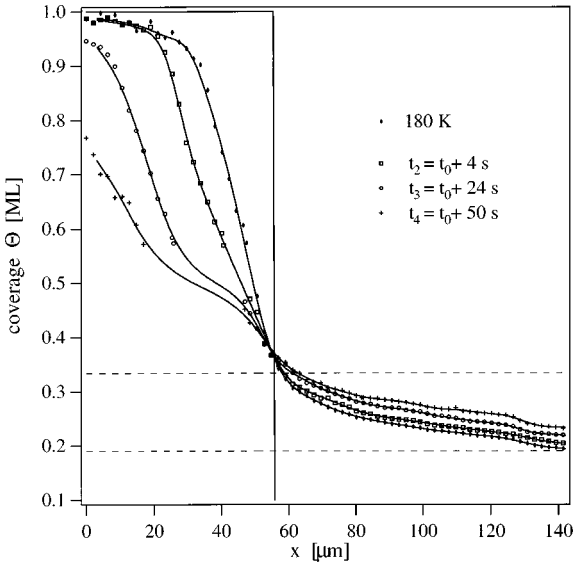

FIG. 3. Concentration profiles obtained for different times at $T=195$ K (including that at $T=180$ K).

brightest parts of the image signify intermediate coverages. As discussed previously,[7] potassium diffusion proceeds along terrace structures on the surface, giving rise to the ''streamers'' apparent in Fig. 1. This quasi-one-dimensional diffusion is confined by step bunches or even totally blocked by defect structures. (The development at the defect site roughly in the center of Figs. 1a–d presents a characteristic example.) It should be noted that in the case of the particular area of the surface selected for the images in Fig. 1, the streamers are preferentially directed normal to the strip edge. On other regions of the substrate, where the terrace orientation is roughly parallel to the strip, however, virtually no diffusion is observed below the temperature at which diffusion over the steps begins.

Figures 1b–d show a selection of PEEM images demonstrating the temporal evolution of the potassium distribution at 195 K. The intensity profiles of the particular streamer indicated by the white line between A and B are displayed below the respective images. The intensity maximum broadens with time and develops into a plateau indicating that there is a region of constant coverage in the diffusion zone, a feature incompatible with a diffusion coefficient independent of concentration. For the quantitative analysis of these data the intensity profiles have to be converted into concentration profiles. The problem which arises here is connected with the minimum in the work function curve which inevitably gives two concentration values in certain parts of the work function, i.e., intensity, range. Our approach for overcoming this difficulty is illustrated in Fig. 2. For a particular intensity profile (curve on the left in Fig. 2) we know that the region from $x=0$ to the maximum corresponds to the coverages given by the right hand branch of the work function curve (see Fig. 2). Since it was found in the calibration described above that the intensity follows the work function curve almost exactly, every data point along x is easily converted into the related concentration. The analogous procedure can be applied for coverages below that of the work function minimum by taking the left hand branch of the work function curve. The resulting two-part concentration profile is shown as the curve on the right in Fig. 2. The critical region of coverage is obviously around the minimum because $d\Theta/d(\Delta\varphi)\rightarrow\infty$ and the coverage between about 0.45 and 0.55 ML can no longer be correlated with a distance. From the shape of the reliably determined parts of the concentration profile it is, however, evident that the curve must go through a point of inflection in the missing interval. To avoid any artificial features the whole curve was fitted with cubic spline functions, thus interpolating in the gap with a curve of minimum curvature. This rather conservative approach assures that any features connected with this part of the concentration profile will be ''underestimated.'' The set of concentration profiles used in the following Boltzmann–Matano analysis is shown in Fig. 3; the lines connecting the data points represent the spline function fits.

B. Boltzmann–Matano transformation and calculation of *D*

The fact that the concentration profiles in Fig. 3 can be determined along such a streamer is proof that the spreading of potassium occurs essentially via a one-dimensional way. We thus feel justified in analyzing the profiles with the one-dimensional form of the diffusion equation:

$$\frac{\partial\Theta(x,t)}{\partial t}=\frac{\partial}{\partial x}\left(D(\Theta)\frac{\partial\Theta}{\partial x}\right). \tag{1}$$

Employing the Boltzmann–Matano method,[2,16] which allows the diffusion coefficient D to be concentration-dependent, it has been shown that the diffusion equation can be converted into the ordinary differential equation

$$-\frac{\eta}{2}\frac{d\Theta(\eta)}{d\eta}=\frac{d}{d\eta}\left(D(\Theta)\frac{d\Theta}{d\eta}\right) \tag{2}$$

by the variable transformation

$$\eta=\frac{x}{\sqrt{t}},$$

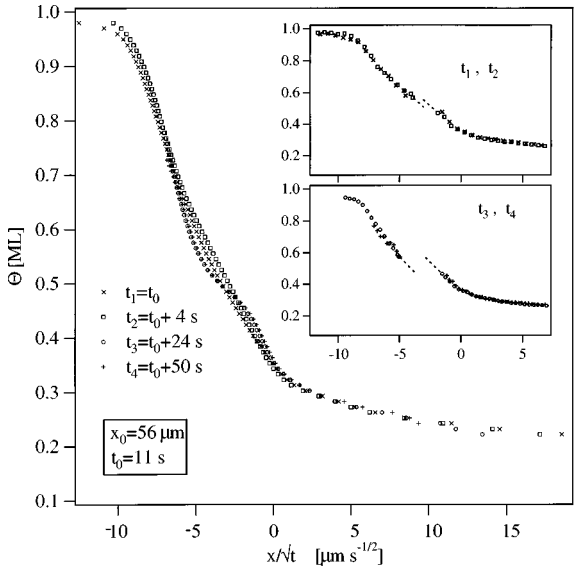

FIG. 4. Reduced concentration profiles Θ vs η. The determination of the initial parameters x_0 and t_0 is described in the text. The insets show the unsmoothed data points of the t_1/t_2 and t_3/t_4 profiles.

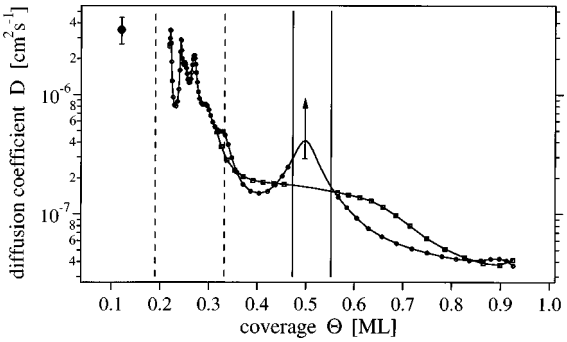

FIG. 5. Coverage dependence of the diffusion coefficient $D(\Theta)$ obtained after times t_2 (open squares) and t_3 (open circles) from the corresponding concentration profiles. In the low coverage regime diffusion is strongly influenced by defects giving rise to a large scatter. The value of the diffusion coefficient at $\Theta=0.12$ ML (filled circle) has been determined previously with a different technique, Ref. 9.

provided that the diffusion coefficient depends only on Θ. The initial and boundary conditions require at $t=0$ a concentration distribution which corresponds to an infinitely extended step function with the edge located at $x=0$ and $\Theta=\Theta_0$ for $x<0$ and $\Theta=0$ for $x>0$. By integration of (2) the following expression for $D(\Theta)$ is obtained:

$$D(\Theta^*)=-\frac{1}{2t}\frac{dx}{d\Theta}\bigg|_{\Theta^*}\int_0^{\Theta^*}x\,d\Theta, \tag{3}$$

yielding the diffusion coefficient at a particular coverage Θ^*. The initial and boundary conditions are valid in our experiment as long as all profiles considered extend up to 1 ML which would, strictly speaking, exclude the profile at t_4 from the analysis. The location of the initial step, $x=0$, for a measured profile is crucial for the calculation of the integral in (3). It is usually determined by choosing its location at the experimental curve by requiring that

$$\int_0^{\Theta_0}x\,d\Theta=0 \tag{4}$$

which just describes the particle conservation. In our treatment we use a different approach which can be considered as a necessary and sufficient condition for the applicability of the Boltzmann–Matano method. If the concentration is only a function of η, it must be possible to reduce all measured profiles to just one curve by using the scaled variable η. Since neither $x_0\equiv x=0$ nor $t_0\equiv t=0$ can be directly determined from the experiment, a least squares fit of the profile curves versus η was performed treating both x_0 and t_0 as free parameters. The fact that the curves in Fig. 4 are all coincident clearly justifies—within the experimental error—an analysis using the Boltzmann–Matano method. In fact, a total of 9 concentration profiles measured between t_1 and t_4 were used for fitting, although only a representative selection is shown in Fig. 4 in order to keep the drawing simple. The resulting position x_0 (indicated at $x=56$ μm in Fig. 3) agrees rather well with the border of the initial strip extrapolated from sample regions where more defects block the diffusion and the edge remains more clearly visible. The value of $t_0=11$ s also appears reasonable in view of the experimentally necessary delays in setting the temperature. Upon closer inspection of the reduced curves, it is apparent that the flatter portion develops with time but does not change much after $\approx$20 s, i.e., the t_3 and t_4 curves are almost identical. To demonstrate the difference in the shape of the curves the insets show the raw data points for small and large t as derived with the procedure described above. The gap between the two branches of the concentration profile increases with time and thus the slope at the corresponding points in the profile must also increase. This effect is clearly visible for the curves in the main figure where the points shown have been derived from the interpolated curves in Fig. 3. Since these effects appear on the reduced Θ versus η curves, it must be concluded that the diffusion coefficient changes with time in the initial stages of diffusion. In order to compute the integral in Eq. (3) we have linearly extrapolated the concentration profiles for the diffusion distances beyond the imaged region (x between 140 and 260 μm). That this somewhat crude estimate works quite well can be verified by checking whether particle conservation [Eq. (4)] conforms with the location of x_0 as derived above. Moreover, the calculated value of $D(\Theta^*)$ depends predominantly on the derivative $dx/d\Theta$ for $\Theta^*>0.2$, whereas the estimated part of the integral contributes only a constant offset.

A D versus Θ dependence characteristic of the stationary state reached after $\sim$20 s is shown by the open circles in Fig. 5. Although the curve has been computed from the particular profile measured at t_3 (see Figs. 2 and 3) all the curves obtained after a similar elapse of time (also from other streamers) agree well with this result within experimental error. In the higher coverage region, the concentration profiles have been analyzed as far as reliable data points were available. The t_4 profile, for instance, is only used for the $D(\Theta)$ calculation up to about 0.75 ML. In the coverage region above $\sim$0.33 ML $D(\Theta)$ decreases monotonically with a superimposed maximum at 0.5 ML. The large scatter of D values between 0.2 and 0.33 ML reflects the presence

of defects on the streamer. Because the coverage decrease is only gradual in that part of the streamer (see Fig. 3), these defects cause large variations in the derivative [Eq. (3)], and thus in D, although the profile itself is only weakly affected. The most prominent defect visible as a concentration step in Fig. 3 at ~ 0.26 ML and $x \sim 130$ μm can be easily correlated with the minimum in Fig. 5 at this coverage. The single data point at 0.12 ML (filled circle in Fig. 5) shows the value of D at 195 K as derived from our previous study[9] where both the pre-exponential factor and the activation energy of D were determined with a different method of analysis. The relatively good agreement with the results obtained here indicates that the diffusion coefficient below 0.2 ML is approximately constant or at most changes only slightly with coverage. The arrow at 0.5 ML expresses the uncertainty in D which arises from the fact that there is some ambiguity in the functions interpolating the missing part of the concentration profile at the point of inflection. It should be noted, however, that the lower end of the arrow corresponds to the quite unrealistic straight line interpolation in the gap. Even in this limiting case the diffusion coefficient has a maximum at 0.5 ML. Unfortunately, the absolute peak height cannot be determined precisely from our experiments. The open squares give the $D(\Theta)$ dependence as derived from the t_2 profile assuming Eq. (3) to be valid. The maximum in the diffusion coefficient appears to be smeared out over a greater concentration range than for the stationary case.

IV. DISCUSSION

Diffusion of electropositive metals, such as alkali or alkali-earth metals, on single crystal surfaces has been found to exhibit a richly structured dependence of the diffusion coefficient on coverage in almost all the systems studied so far.[12] D can in fact vary over several orders of magnitude. Although the largest oscillations have been observed for multilayer diffusion, some adsorption systems also show maxima and minima in the sub-monolayer regime at specific coverages.[11] As a rule, these features appear to be related to phase transitions in the adlayer. The same applies to the system investigated here: the diffusion coefficient peaks in that coverage interval where in LEED a $p(2\times 2)$ pattern is visible, i.e., the adlayer forms its own lattice. An explanation for this correlation is based on the fact that (in the generalized Darken approximation[17]) the chemical diffusion coefficient can be divided into an effective jump rate Γ and a thermodynamic factor:[18]

$$D = \Gamma \cdot \frac{\partial(\mu/kT)}{\partial \ln \Theta} \quad \text{with} \quad \Gamma = \Gamma_0 \cdot e^{-E/kT}, \tag{5}$$

where Γ is the thermal average of the transition rate. Even though both factors are coverage-dependent, we expect the thermodynamic factor to dominate close to a phase transition.[19] It has been shown (see for example Ref. 1) that the thermodynamic factor is inversely proportional to the thermally driven relative concentration (coverage) fluctuations

$$\frac{\partial(\mu/kT)}{\partial \ln \Theta} = \left(\frac{\langle \Delta c^2 \rangle}{\langle c \rangle} \right)^{-1}, \tag{6}$$

where $\langle\ \rangle$ refers to the thermal average. If the adsorbed particles form a perfect ordered array these fluctuations should be smallest; the thermodynamic factor and hence the diffusion coefficient should exhibit a maximum. Below or above the coverage corresponding to the ordered array either vacancies must be present or interstitial sites in the adlayer lattice must be occupied and the fluctuations in local concentration increase, i.e., the diffusion coefficient decreases. This dominant role of the thermodynamic factor has been confirmed by Monte-Carlo simulations on a square lattice in which the formation of an ordered layer had been realized through nearest and next-nearest neighbor interactions.[19–21] An interpretation along these lines has also been used to discuss the maximum in the diffusion coefficient in the systems W{110}-O, which is concomitant with the formation of a (2×1) overlayer,[3] and Ge{111}-Ag.[4]

On the other hand, there is evidence that the occurrence of an ordered overlayer may also be connected with a minimum in the diffusion coefficient. For a Pb layer on Cu{100} the diffusion coefficient passes through a local minimum for Θ between 0.3 and 0.4 where a $c(4\times 2)$ LEED pattern is observed.[22] By modelling this system with Monte-Carlo simulations that included nearest neighbor repulsive interactions these authors actually obtained the expected maximum in the thermodynamic factor at $\Theta = 0.5$, corresponding to a $c(2\times 2)$ ordering of the adlayer. At the same time, however, a pronounced minimum in the jump rate Γ was found to dominate and in effect leads to the observed minimum in $D(\Theta)$.

An illustrative microscopic picture as to how a plateau-like region in the concentration profile can emerge is given by the ''unrolling carpet'' mechanism.[23] Particles moving from the higher concentration region into the area where the ordered phase exists have to occupy interstitial sites of the adlayer lattice which are energetically less favorable. In consequence, they cross this region with increased mobility until they arrive at those parts of the concentration profile where vacancies can be filled. Thus, the coverage corresponding to the ordered phase is dynamically stabilized and the region it covers increases during the evolution of the concentration profile. The unrolling carpet description assumes of course that a certain part within the profile is already ordered. The question which then arises concerns the initial formation of an ordered region in a steep initial profile. The results presented here show that the formation of the flat portion in the concentration profile corresponding to the peaked $D(\Theta)$ curve is preceded by a stage in which a weaker, substantially broadened maximum in D occurs. Apparently, a minimum critical area of ordered phase is required to sustain a constant coverage region. We can only speculate as to the structural composition of the diffusion profile at this stage. One possibility may be that patches, or islands, of the ordered phase are surrounded either by dilute or by more concentrated regions with the result that the effective concentration is either above or below the critical coverage. Hence, the apparent diffusion coefficient increases. This description would mean

that there are localized states of the layer far from equilibrium. The existence of such a state would question the widely used assumption of strictly local equilibrium over the whole profile, which in turn underlies the concept of the thermodynamic factor.

Apart from the peak maximum the diffusion coefficient appears roughly constant below 0.25 ML and then decreases smoothly with increasing coverage up to saturation. Since the interaction within an alkali metal layer is repulsive this behavior of the diffusion coefficient seems to contradict the predictions of theoretical treatments in which an overall increase of D with coverage is obtained for repulsive interactions. It must be noted, however, that such lateral interactions are modelled in almost all cases by nearest or next-nearest neighbor two particle potentials which are suitable for quasi-chemical approximations or Monte-Carlo simulations. The dipole–dipole interaction predominant in alkali metal layers is certainly of long range character and, moreover, changes with coverage. Alkali metal atoms are thought to donate nearly one electron to the metal at low coverages forming ionized adatoms which in combination with the related image charges interact repulsively. In an alternative picture the alkali metal atom becomes strongly polarized as a result of a covalent interaction with the substrate. As the coverage increases, the charge donation (or polarization) decreases due to the dipole–dipole depolarization in the adlayer; at the same time, the mean particle–particle distance also decreases. This complex interplay of effects is mirrored in the almost universal curve for the decrease in work function as a function of coverage (Fig. 2, center). In the present system, we attribute the overall decrease of the diffusion coefficient to the depolarization of the K atoms which in effect reduces the repulsive interaction and thus the diffusivity. In the lowest coverage regime no depolarization occurs (as apparent from the initially linear decrease of the work function) and, because of the rather large particle–particle distance, the diffusion coefficient remains roughly constant.

The only closely related investigation we are aware of has been performed on the Ru{001}-K system.[24] By application of laser-induced thermal desorption (LITD) the diffusion coefficient was determined as a function of coverage and found to increase by more than two orders of magnitude between half and full saturation coverage. Although the sequence of ordered phases is nearly identical for Pd{111}-K and Ru{001}-K [$p(2\times2)$ and $(\sqrt{3}\times\sqrt{3})$R30° LEED patterns] there is no indication of phase transition induced features in the $D(\Theta)$ curve in Ref. 24. The most plausible reason for these discrepancies is in our view connected with the fact that the experimental signal used in LITD quantifies the number of particles which diffuse over a definite time interval into a thermally depleted area. Neither concentration profiles are measured nor, most importantly, is the detailed substrate topography in this area probed. As the diameter is typically of the order of 100 μm (see Fig. 1 for a comparison) the diffusion coefficient determined then represents most probably a defect-averaged quantity. Moreover, the temperatures used in Ref. 24 to produce reasonable signals were in the range of 200 K and above. From the PEEM images we have observed in our experiments that diffusion across steps already commences at 205 K. A clear indication that the processes measured in the two studies may not be comparable is found in the measured activation energies. While in Ref. 24 the lowest coverage value is given as $E_a=390$ meV, we have recently determined an activation energy of 66 meV in the system Pd{111}-K at low coverage.[9] We feel more attention must be paid to substrate topography in order to account for the discrepancies between surface diffusion studies prevalent in the literature.

In the study presented here we have used only the most defect-free streamers for the analysis and are quite confident that the obtained values for the diffusion coefficient represent essentially those of the ideal surface. Fortunately, defects located on a streamer are revealed by breaks in the slope of the concentration profiles (see, for example, the location $x\approx130$ μm on the curves in Fig. 3) and thus can be accounted for by either rejecting the whole streamer or omitting these sections. In the same way, linear defects crossing a streamer are easily identified on the substrate (for such cases, see Refs. 6 and 7).

V. CONCLUSIONS

Photoelectron emission microscopy (PEEM) has been used to monitor the evolution of concentration profiles of potassium diffusing from an area initially covered with a monolayer of the alkali metal on a Pd{111} surface. The coverage dependence of the diffusion coefficient $D(\Theta)$ has been evaluated via a Boltzmann–Matano analysis. The diffusion coefficient decreases with Θ between 0.2 and 1.0 ML but exhibits a local maximum at $\Theta\sim0.5$ ML which corresponds to the formation of a $p(2\times2)$ superstructure. The decrease of D with increasing Θ is ascribed to the well-known depolarization effect occurring at alkali metal layers. The local maximum at $\Theta\sim0.5$ ML is attributed to a maximum in the thermodynamic factor induced by an order–disorder phase transition.

ACKNOWLEDGMENTS

M.S. would like to thank the Max-Planck-Gesellschaft for a studentship. The work has been supported by the Deutsche Forschungsgemeinschaft through Sonderforschungsbereich 290 and the Grant Agency of the Czech Republic under the Grant No. GA AVCR#A1010718.

[1] R. Gomer, Rep. Prog. Phys. **53**, 917 (1990).
[2] C. Matano, Jpn. J. Phys. **8**, 109 (1933).
[3] R. Butz and H. Wagner, Surf. Sci. **63**, 448 (1977).
[4] E. Sigula and M. Henzler, J. Phys. C **16**, 1543 (1983).
[5] R. H. Milne, M. Azim, R. Persaud, and J. A. Venables, Phys. Rev. Lett. **73**, 1396 (1994).
[6] M. Ondřejček, W. Stenzel, H. Conrad, V. Cháb, Z. Chvoj, W. Engel, and A. M. Bradshaw, Chem. Phys. Lett. **215**, 528 (1993).
[7] M. Ondřejček, V. Cháb, W. Stenzel, M. Šnábl, H. Conrad, and A. M. Bradshaw, Surf. Sci. **331–333**, 764 (1995).
[8] Adsorbate coverages used here are referred to saturation of the potassium layer, i.e., $\Theta=1$ ML corresponds 0.33 K atoms per substrate atom.
[9] M. Šnábl, M. Ondřejček, V. Cháb, W. Stenzel, H. Conrad, and A. M. Bradshaw, Surf. Sci. **352–354**, 546 (1996).
[10] J. Ellis and J. P. Toennies, Phys. Rev. Lett. **70**, 2118 (1993).
[11] A. G. Naumovets, V. V. Poplavsky, and Yu. S. Vedula, Surf. Sci. **200**, 321 (1988).

[12] A. T. Loburets, I. F. Lyuksyutov, A. G. Naumovets, V. V. Poplavsky, and Yu. S. Vedula, in *Physics and Chemistry of Alkali Metal Adsorption*, edited by H. P. Bonzel, A. M. Bradshaw, and G. Ertl (Elsevier Science, B.V., 1989).
[13] A. Berkó and F. Solymosi, Surf. Sci. **187**, 359 (1987).
[14] G. Pirug and H. P. Bonzel, Surf. Sci. **194**, 159 (1988).
[15] M. Kiskinova, G. Pirug, and H. P. Bonzel, Surf. Sci. **133**, 321 (1983).
[16] J. Crank, *The Mathematics of Diffusion*, 2nd ed. (Clarendon, Oxford, 1975).
[17] R. Ferrando, E. Scalas, and M. Torri, Phys. Lett. A **186**, 415 (1994).
[18] D. A. Reed and G. Ehrlich, Surf. Sci. **102**, 588, 603 (1981).
[19] G. E. Murch, Philos. Mag. A **43**, 871 (1981).
[20] A. Natori and H. Ohtsubo, Surf. Sci. **171**, 13 (1986).
[21] C. Uebing and R. Gomer, J. Chem. Phys. **95**, 7626 (1991).
[22] C. Cohen, Y. Girard, P. Leroux-Hugon, A. L'Hoir, J. Moulin, and D. Schmaus, Europhys. Lett. **24**, 767 (1993).
[23] A. G. Naumovets and Y. S. Vedula, Surf. Sci. Rep. **4**, 365 (1985).
[24] E. D. Westre, D. E. Brown, J. Kutzer, and S. M. George, Surf. Sci. **294**, 185 (1993).